SATCOM RX/TX USER TERMINAL ANTENNAS WITH INTELLIGENT PIXELS

Luigi Boccia (1), Alireza Shamsafar (1), Emilio Arnieri (1), Ali Imran Sandhu (1), Giandomenico Amendola (1), Tatyana Purtova (2), Xiaolei Gai (2), Václav Valenta (2), Hermann Schumacher (2), Wolfgang Menzel (2), Erika Meniconi (3), Kaynak Mehmet (4), Bernd Tillack (4), Volker Ziegler (3)

(1) Università della Calabria, Università della Calabria, DEIS Via Bucci, 41 D 87036 Rende (Italy),

E-mail: luigi.boccia@unical.it

(2) Universität Ulm

Albert-Einstein-Allee 41, 89081 Ulm – Germany

(3) EADS Innovation Works

Willy-Messerschmitt-Str., 85521Ottobrunn – Germany

(3) IHP - Innovations for High Performance Microelectronics

Im Technologiepark 25 15236 Frankfurt (Oder) - Germany

ABSTRACT

This work presents an innovative configuration of reconfigurable Ka-band Tx/Rx SatCom user terminal antenna operating in the 29.5–30.8GHz and 19.7–21.0GHz bands. The proposed approach is based on a low-profile active phased-array implemented integrating a multilayer printed circuit with reconfigurable SiGe BiCMOS MMICs. The radiating part of the array is implemented employing dual band elements arranged in an interleaved configuration. Each radiating element is equipped with one complete Tx/Rx unit. Chips developed for this project are referred to as "intelligent pixels" as they integrate all the RF analogue, mixed-signal and digital control circuitry. Each pixel comprises multiple Tx and Rx cores which can independently operate amplitude and phase control, as it is required to implement 2-D beam steering arrays. Furthermore, power amplifiers and low noise amplifiers are embedded into each transmit and receive core respectively to fulfill link budget requirements for Sat-Com applications. In the proposed configuration, each SiGe BiCMOS MMIC chip controls 2 Rx and 4 Tx antenna elements. Each multi-core chip is accessible via a common serial I^2C bus which enables full control over the array with limited control lines. Chip reconfigurability can be enhanced through fully monolithically integrated RF-MEMS switches.

I. INTRODUCTION

In the last few years, there has been a growing interest for Sat-Com mobile multimedia applications requiring high quality services and global coverage [1]. In this context, one of the most critical aspect is related to the development of the phased-array antenna system [2], [3]. Indeed, antenna requirements for Sat-Com user terminal are usually very challenging [4]. Typically, it is required beam scanning over very wide angles, low interactions with the environment, dual band (Tx and Rx) operation, low-cost and low-profile.

In the most typical approach, these requirements are satisfied by employing two separated radiation apertures for the Rx and Tx channel. [5] Pointing of the two dual-polarized antennas is usually mechanical in azimuth and electronically steered in elevation [6]. This approach results in a complex antenna architecture which can be hardly mounted on vehicles or airplanes without affecting their aerodynamic and aesthetic profile. Furthermore, the cost of this solution remains high even for mass production. Arrays with full electronic beam scanning were proposed using customized GaAs MMICs [7], [8]. Although this is a step in the right direction, it is still not eanough to greatly reduce the cost of the user terminals. Indeed, independent silicon chips will be required to control Tx and Rx modules and it is not possible to integrate multiples cores in the same MMIC with high yield.

This paper introduces a new configuration of Ka SatCom user terminal antenna as it is being developed within the framework of the European FP7 project Flexwin [9]. The proposed configuration is based on highly reconfigurable RFIC components referred to as "intelligent pixels" combined with a quasi-planar antenna array. Each element of the array is therefore integrated with a multicore chip developed on the SiGe BiCMOS technology, where amplitude and phase control elements are integrated with environmental sensing and digital controls controlled through a I^2C bus.

In terms of reconfigurability, this approach proposes to achieve a significant advance towards smart RF micro-systems enabling the realization of highly reconfigurable and multifunctional millimetre-wave building blocks which can be integrated with environmental sensing blocks and with digital controls.

Even if the availability of multifunctional chips reduces the complexity of the phased array, the design of the passive parts of the phased array is also critical especially if a single radiating aperture is employed for dual band

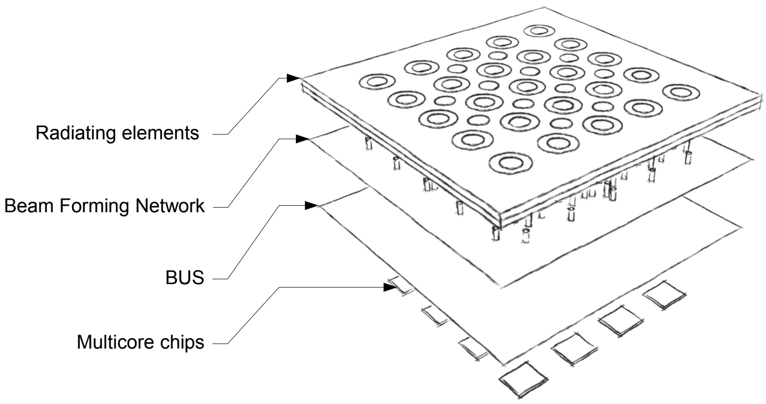

Figure 1. Conceptual layout of the SatCom user terminal antenna with "intelligent pixels": exploded view.

operation. In this paper, it is also introduced an interleaved configuration implemented through printed annular slots embedded into a via cage which reduces surface wave losses.

II. ARRAY ARCHITECTURE

The proposed approach is based on the concept of low-profile active phased array, which targets the above mentioned objectives by combining the 2-D electronic beam-steering architecture with Tx/Rx units behind each radiating element based on a low-cost semiconductor (SiGe) technology. The potential industrial implementation is clearly a lower cost alternative compared to other existing active phased array antennas. Moreover, the integration in the same chip of both RF and digital components is a clear advantage with respect to GaAs-based designs. In addition, the quasi-planar (height less than 5cm) integration of these antenna types will produce almost no additional drag while the use of a single radiation aperture for both Tx and Rx bands will further reduce the size of the array.

A conceptual layout of the proposed configuration is shown in Fig. 1. The whole array structure is built making use of multilayer Printed Circuit Boards (PCBs). Various types of metalized via holes and bonding techniques are used to connect different layers. A single radiating board hosts both the Tx (30GHz) and Rx (20GHz) array elements in an interleaved arrangement. Details on the radiating elements will be given in next section.

Multicore chips are wire-bonded to the lowest layer. Each chip can be used to connect 4 Tx modules and 2 Rx modules. Each module includes amplification and phase control stages. Each module is connected to an array element and on-chip combining and switching stages are employed to merge different signals into a single chip output. A lower metal layer implements a serial bus structure which is used to control and reconfigure the on-chip analogue RF components. The output port of each chip is combined by means of a wide-band Beam Forming Network (BFN) realized in the lowest layer.

The most salient feature of the proposed antenna is the fact that each the radiating element is equipped with one complete Tx/Rx unit realized on a single SiGe BiCMOS RF-MEMS chip. This system-on-chip concept will lead to improved RF-performance of the complete antenna system by distributed amplification in Tx and Rx. Furthermore, individual RF components will be independently reconfigurable through digital controls integrated on the single chip. Additional smart functionalities can be implemented by employing integrated temperature sensors which can be used for self-calibrations and for drift corrections.

A. Array requirements

The proposed array architecture was demonstrated on a partial Direct Radiating Array whose requirements were derived from the full scale model. The specifications of the partial array are:

- Frequencies:

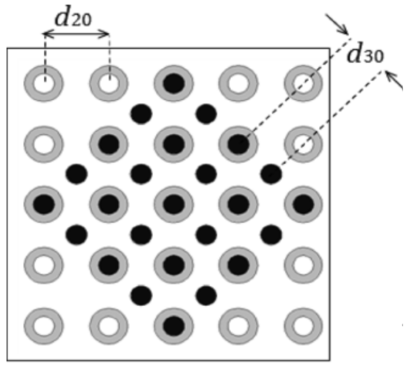

Figure 2. Configuration of the dual band array. Grey rings represents Rx elements and black circle represents Tx elements.

- Receive: 19.7 – 21.0 GHz
- Transmit: 29.5 – 30.8 GHz

- Polarization: linear
- Beam steering: electrical in azimuth and elevation
- Coverage: +/-60 degrees
- Height: 5cm
- Total output power per element: 40mW
- Number of elements: approximately 100
- Receiver noise figure per element: 5dB

III. RADIATING BOARD

The main issue in the implementation of a dual band array for Ka SatCom user terminals is related to the large separation between the two operating frequencies. In the proposed configuration, the high wavelength difference can be balanced by interleaving dual-band elements with single-band antennas operating at the higher frequency. A schematic view of the proposed arrangement is shown in Fig. 2. The 20 GHz (Rx) and 30 GHz (Tx) elements are placed concentrically and nested one into the other. This choice results in a configuration where two arrays, one Rx and the other one Tx, are integrated on the same aperture with their principal axis rotated of 45 degree one respect to the other. The 45 degree inclination allows for a separation between radiating elements which is almost equal at the two frequency bands. As an example if $d_{20}=0.5\lambda_{20}=7.5\text{mm}$ then one has that $d_{30}=0.533\lambda_{30}=5.33\text{mm}$.

A. Antenna element structure

Two antennas, one operating around 20 GHz (type I) and the other at 30 GHz (type II), were studied and designed. Fig. 3 show the antenna operating at 20GHz (type I). The annular slot has an inner radius of 1.8 mm and the outer one 2.7 mm. The antenna is fed with a stripline entering the via shield. To reduce the size and enlarge the bandwidth the outer border of the antenna was meandered with the use of ridges. The inner border of the annular slot is also grounded with vias forming a coaxial structure. The inner part of the structure can be used to host circuitry or to accommodate another antenna operating at higher frequency. In Fig. 4 a 30GHz radiator (type II) is shown with inner radius 1mm and the outer one 1.51mm. In this last case the radiator is fed by means of a slot on the ground plane excited with a stripline. Differently from the first case a single via has been used as inner conductor of the coaxial structure.

The two antennas can be combined to form a dual band radiator for Rx/Tx application at Ka band, In this case the dual band element is designed to operate in the commercial Ka satellite band. The dual band radiator is shown in Fig. 5. The 20 GHz (Rx) and 30 GHz (Tx) elements are placed concentrically and nested one into the

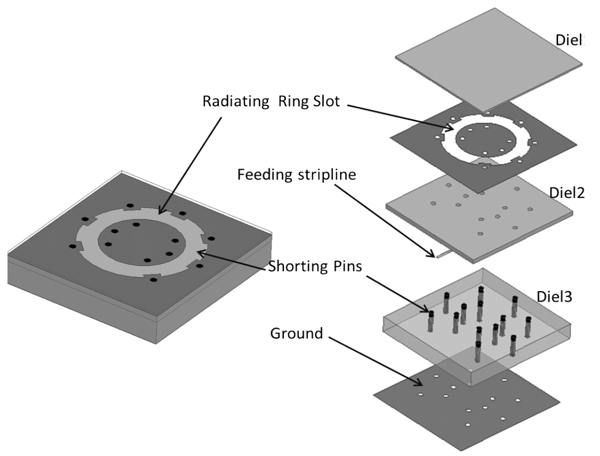

Figure 3. Type I antenna structure. Diel1: DK 3.2 h= 0.125mm. Diel2: DK 4 h=0.3mm. Arlon Multiclad HF DK 4 h=1.1mm

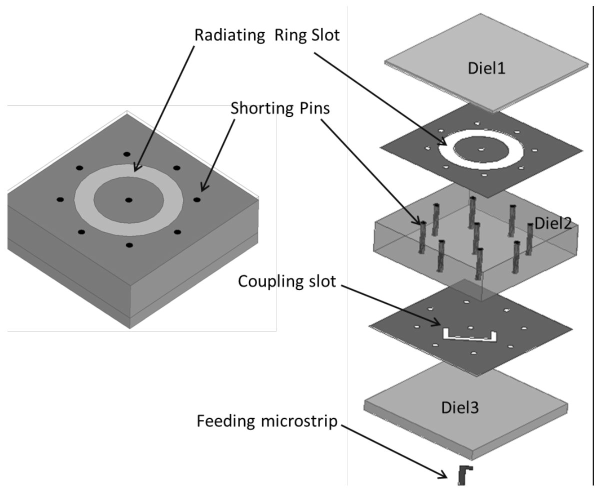

Figure 4. Type II antenna structure. Diel1: DK 4 h= 0.125mm. Diel2: Dk=4 h=1.2mm. Diel3: DK=3 h=0.4mm.

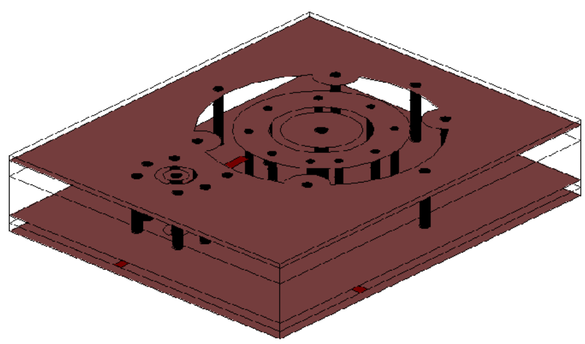

Figure 5. Dual Band radiating element.

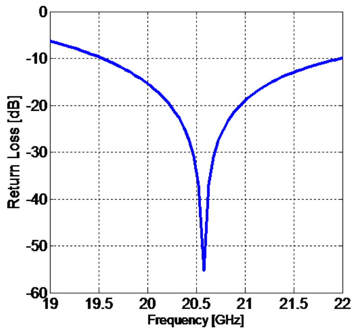

Figure 6. Return Loss of type I antenna

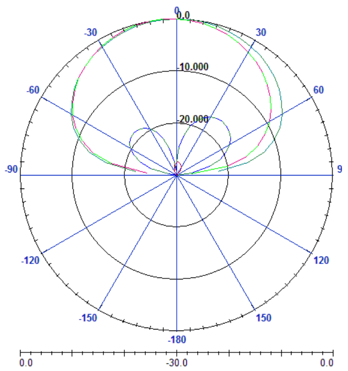

Figure 7. Radiation Pattern (Ex-Ey) of type I antenna computed at 20 GHz.

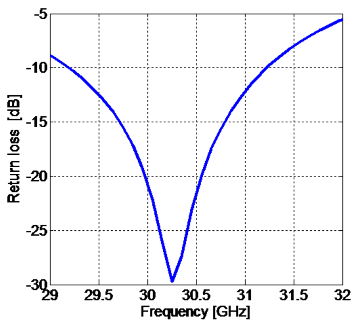

Figure 8. Return Loss of type II antenna

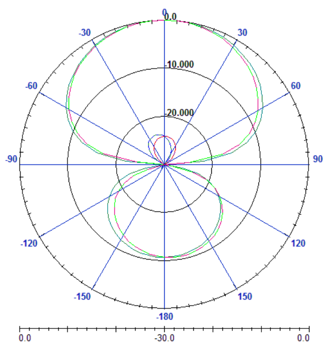

Figure 9. Radiation pattern (Ex-Ey) of type II antenna computed at 30 GHz.

other. The lower frequency radiator is fed with a stripline inserted into the waveguide and the higher frequency element is coupled to a microstrip by means of a slot on the ground plane. The stripline feeding the 20 GHz element is brought to the lower layer by means of a quasi-coaxial structure. The inner and outer radiators are fed at an angle of 45 degree in view of the application to a phased array with a single radiating surface operating on the two frequency bands.

B. Simulation results

The antenna have been designed and simulated with the help of HFSS software [10]. Simulated radiation characteristics of the two isolated radiators are presented in Fig. 6-9. In particular, in Fig. 6 is shown the simulated return loss at the input port of the type I element. As it can be observed, a good match is obtained over a bandwidth of 2.5GHz. In Fig. 7 the normalized antenna radiation patter calculated at 20 GHz is reported. As it can be seen, the antenna has a good radiation characteristics with low cross-polar radiation. In Fig. 8 is reported the simulated return loss for type II antenna which shows a 2 GHz bandwidth. Fig. 9 shows the radiation diagrams of the antenna at 30 GHz. It is worth noticing that the back radiation now visible in the antenna pattern will be

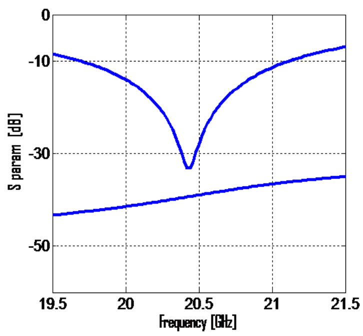

Figure 10. Scattering parameters of the dual band antenna in the Rx band.

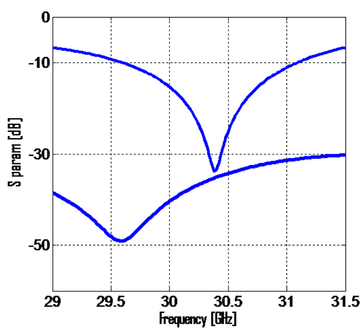

Figure 11. Scattering parameters of the dual band antenna in the Tx band.

shielded by lower metallic layers in the final array arrangement.

In Fig. 10 and 11 the scattering parameters of the dual band element are reported. In both the Rx and Tx cases bandwidth is of about 1.3GHz. Isolation between the elements is good staying well below 30dB over all the covered band. For all the antennas presented in this paper Gain is in a range between 5 and 6 dB in the whole operating bandwidth.

IV. CHIP CONFIGURATION

The interleaved architecture of the array results in a high number of elements to be fed through the distribution network which can thus result very critical because it requires high number of power dividing and combining stages. A further element of complexity derives from the fact that the array elements in the two bands is not equal and not uniform. Indeed, different number of elements should be required in the two bands. Specifically, in the final array the Tx elements will be more dense than the Rx cells in the central area whereas only Rx cells will be located in the array periphery. The most obvious solution is to use a single reconfigurable Rx and Tx chip connected to each element. However, this would make the integration of such a high number of chips complex and critical and it would make very the layout of the distribution network very complex.

As a possible solution, we propose the use of a multi-core chip which is schematically shown in Fig. 12. Each chip contains by four Tx elements and two Rx elements. The hexa-chips are accessible via a common serial I^{2}C bus carrying clock (SCLK), reset (RST) and bi-directional data (SDATA) signals. Each hexa-chip consists of one I^{2}C core and Tx/Rx modules (Fig. 13). To individually address up to 36 elements of the sub-array, each I^{2}C slave has a unique 6-bit address, defined in the prototype by wire-bonding the address bits to either Vcc or ground.

Each I^{2}C slave has 26 writable (i.e. receiving bits from SDATA) and eight readable (i.e. sending bits to SDATA) registers. Each register is 8-bit (I^{2}C standard). The writable registers serve to reconfigure the hexa-chip between transmit and receive states, to enable/disable DC supply for used/unused ICs to reduce heat dissipation and to set phases and amplitudes of Vector Modulators (VMs). The readable registers contain information provided by on-chip sensors, (e.g. temperature or power level).

Tx/Rx modules of the elementary cell of the Sat-Com user terminal array are schematically shown in Fig. 14. Each Tx core includes a VM and a Power Amplifier (PA) while the Rx cores include a VM and a Low Noise Amplifier (LNA). In order to allow dual operation mode of the array, the hexa-chip should be reconfigured between receive and transmit modes. To this end, the DC-

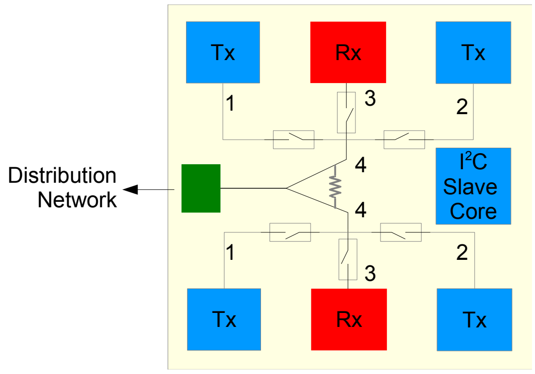

Figure 12. Multicore chip configuration for the Sat-Com user terminal antenna.

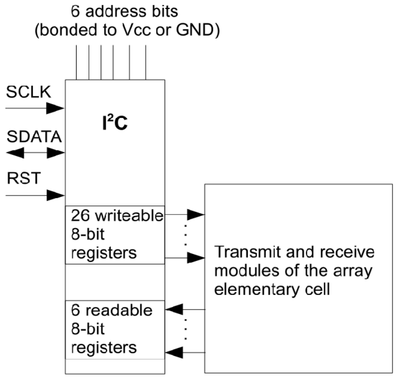

Figure 13. Schematic architecture of the hexa-chip for the antenna array demonstrator. The hexa-chip consist of an I^{2}C slave and Tx/Rx modules of four array unit cells.

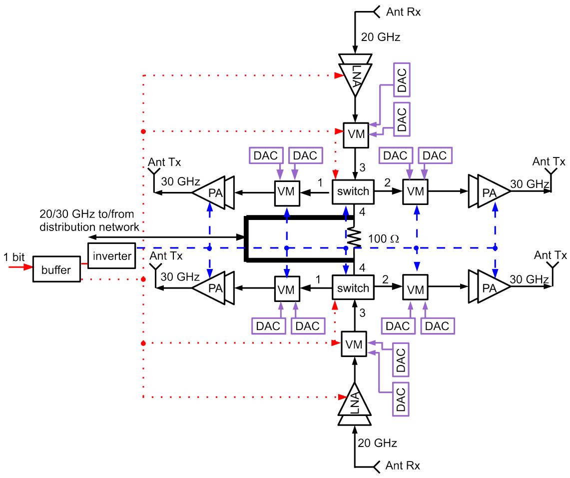

Figure 14. Block diagram of a Tx/Rx module of the transmit array. Dotted red and dashed blue lines show 1 bit signals for bias on/off . Two 8-bit DACs are used to set the vector modulator state.

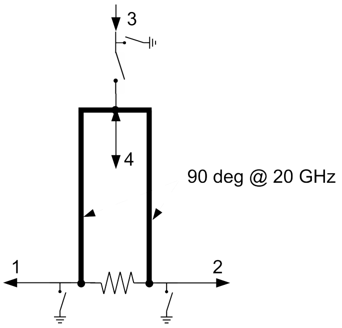

Figure 15. Schematic of the switching network.

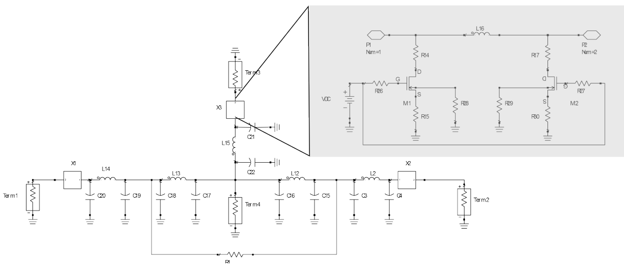

Figure 16. Schematic of the switch network.

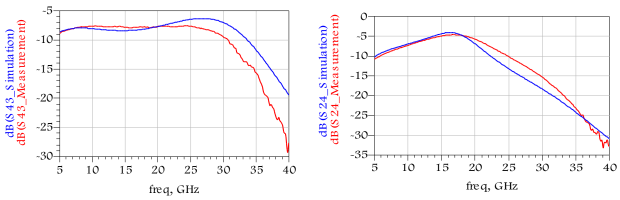

(a) (b)

Figure 17. Simulated and Measured transmission losses of the switch network shown in Fig. 16: a) Tx mode; b) Rx mode.

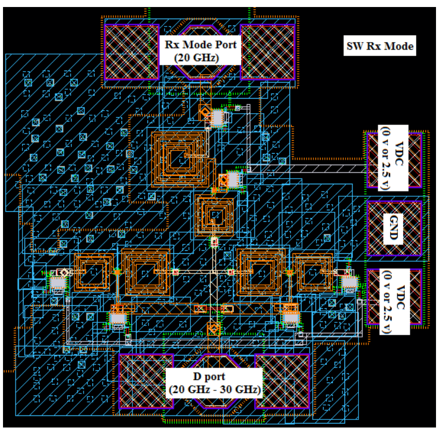

Figure 18. Screen-shot of the switch network layout in the Rx mode.

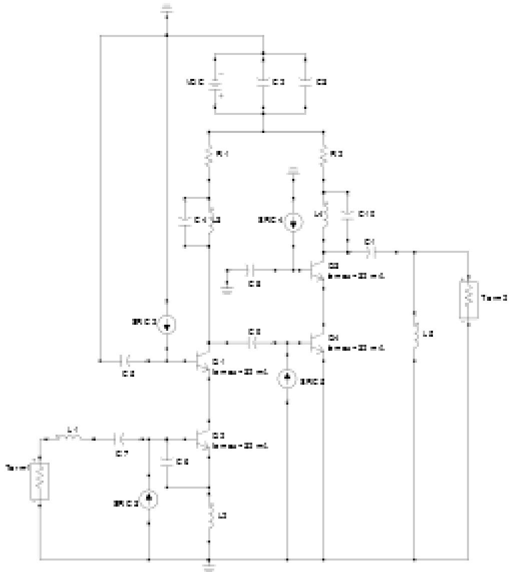

Figure 19. Schematic of the 20 GHz LNA.

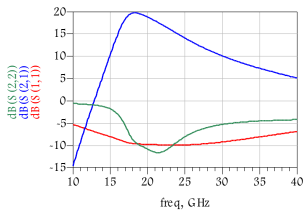

Figure 20.Simulated S-parameters of the 20 GHz LNA.

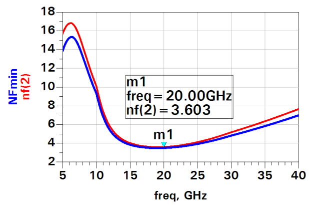

Figure 21.Simulated Noise Figure (NF) of the LNA.

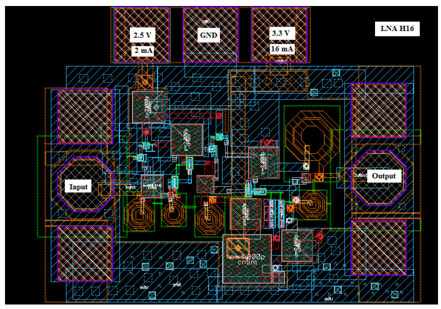

Figure 22. Screen-shot of the final LNA layout. The footprint of the circuit is 0.43×0.55 mm^2.

supply of unused ICs should be switched-off and VMs should be set into the required phase and amplitude state.
In the next subsections, first results on some of the chip components will be reported.
The chip is being designed using the 0.25 µm Si/SiGe BiCMOS technology developed by IHP which offers HBTs with f_T=110GHz and f_{MAX}=180GHz and which allows the integration RF-MEMS switches as shown in [11].

A. Switch network

One of the core elements of the chip is the switch network which is shown in detail in Fig. 15. The node labels 1 to 4 correspond to those in Fig. 14. In the transmit mode, the switches are configured so that the node 4 is connected to the nodes 1 and 2, while the node 3 is disconnected. Thus, the transmit signal present at the node 4 is distributed to the nodes 1 and 2 through the Wilkinson divider. In receive mode, the situation is reversed and node 3 is connected to node 4, while the nodes 1 and 2 are disconnected, i.e. the received RF signal is routed to the node 4.
As shown in Fig. 16, the switch network is based on three high-isolation switches which were implemented by two shunt RFnMOS transistors 150 µm gate width and 0.24 µm gate length. To compensate for the off-state capacitance of the transistors, i.e. to reduce the insertion loss, a series inductor of 190 pH is placed between the transistors. The transistors off-state capacitances and the inductor form a π network, which is matched to 50 Ω. The gate is biased through a 5 kΩ resistor. In addition, a 5 kΩ resistor is placed between the bulk node and ground to reduce insertion loss. The switch network was fabricated and measured. Two different layouts with different pad positions were generated to facilitate the measurement. The layout of the Rx mode configuration is shown in Fig. 18. Simulated and measured transmission coefficients in the two modes are presented in Fig. 17. As it can be observed, simulations and measurements are in good agreement and insertion losses are acceptable in both cases.

B. Low Noise Amplifier

Main requirements of the 20 GHz LNA are a noise figure below 4 dB and gain higher than 20 dB. The schematic of the designed amplifier is shown in Fig. 19. The two-stage cascade configuration was used to meet the high gain requirements. The LNA uses a 3.3 V supply voltage (V_{CC}) for the amplifier core and 2.5 V for bias networks. The collector current (IC) is set to 16 mA to obtain optimal noise figure. Current mirrors are added to improve bias stability over temperature and reduce the impact of variation of the current gain hFE on performance. A degeneration inductor L_2=0.07 nH is used at the emitter of the transistor Q_1 to obtain simultaneous noise and power match by bringing the optimum source reflection coefficient (Γ_0) close to the complex conjugate of S_{11}. The

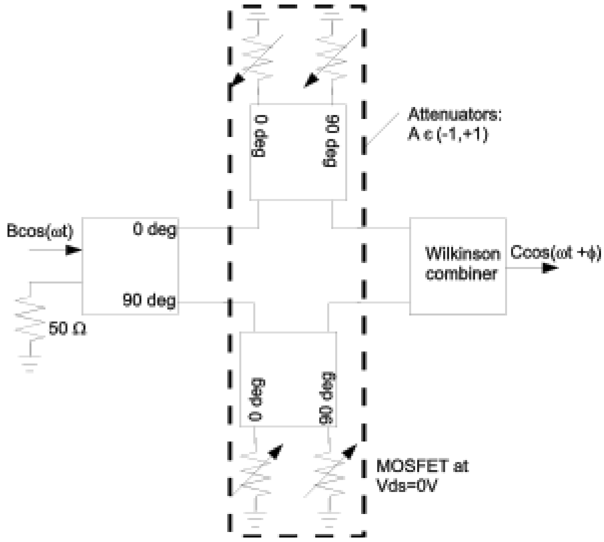

Figure 23. Schematic of the Vector Modulator (VM) with tunable RFnMOS terminations.

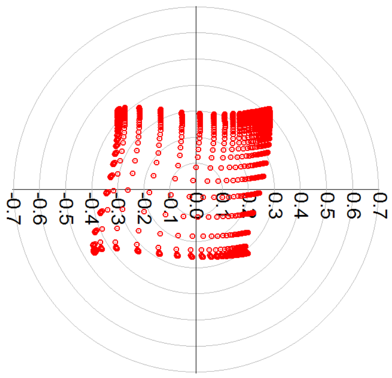

Figure 24. Simulated transmission coefficient of the VM.

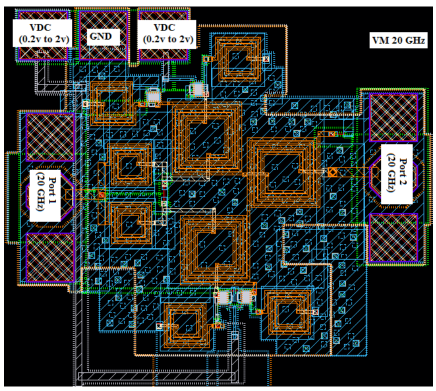

Figure 25. Screen-shot of the VM layout.

value of the inductor L_2 is kept low to avoid gain reduction due to the introduced feedback. The input matching network includes the base inductor L_1=0.15 nH and the base capacitor C_1=1 pF. The output matching network consists of L_5=0.28 nH and C_5=0.152 pF. The collector's load inductors L_2 and L_3 equal 0.13 nH. Both the input and the output are capacitively coupled to prevent DC from affecting adjacent circuitry.

Simulated S-parameters are shown in Fig. 20. At 20 GHz, the gain is around 21 dB. The input and output return losses are below 10 dB. The resulting noise figure is 3.2 at 20 GHz, as shown in Fig. 21. A screen-shot of the final layout is shown in Fig. 22.

C. Vector Modulator

The VM is used to set the amplitude and phase of antenna unit cells. As outlined in Fig. 14, each Rx and Tx chip module will be equipped by a VM. In general, VMs can be realized either as an active or a passive topology. The main advantage of the active approach is low-loss or even gain, depending on the design. On the contrary, passive VMs have losses (in the range of 10 dB). Also, passive topologies do not dissipate DC power, have higher linearity and can be very compact. These advantages were considered of primary importance and, for this reason, the proposed hexa-chips were designed considering a VM topology. The proposed VM is based on vectorial addition of two quadrature bi-phase channels. The schematic is shown in Fig. 23. The gate voltage of RFnMOS transistors should be controlled by 8-bit DACs and the drain-source bias voltage is zero to obtain voltage-controlled resistors tunable between R_{on} and R_{off}, i.e. between few Ω and few kΩ. If the transistor is on, then the reflection coefficient at the drain is close to -1. If the transistor is off, then the reflection coefficient is close to +1. Simulated transmission coefficient is shown in Fig. 24. As it can be observed, a good four-quadrant coverage was obtained. The layout of the VM is shown in Fig. 25.

V. CONCLUSIONS

In this paper we presented a new configuration of Ka band Sat-Com user terminal antenna. The proposed antenna architecture is based on the concept of "intelligent pixel". Each pixel corresponds to an array element including the radiating part and the reconfigurable RF components, controls and even temperature sensors all integrated in the same SiGe BiCMOS chip. This solution allows to individual control each antenna element through a serial bus. Temperature information across the array can be very important for auto-calibration purposes or to correct drift phenomena which can take place in this type of arrays.

As a further feature, the solution introduced in this paper is designed to integrate both the Tx and Rx arrays in the same radiating aperture using dual band elements interleaved with single band elements.

ACKNOWLEDGMENT

This work is funded by the European Union under the project FP7-ICT-2009-5 (FLEXWIN, www.flexwin.eu).

REFERENCES

[1] J. Farserotu e R. Prasad, «A survey of future broadband multimedia satellite systems, issues and trends», *IEEE Communications Magazine*, vol. 38, n°. 6, pagg. 128 –133, Giu 2000.

[2] G. Rebeiz e K. Koh, «Silicon RFICs for phased arrays», *IEEE Microwave Magazine*, vol. 10, n°. 3, pagg. 96 –103, Mag 2009.

[3] D. Parker e D. C. Zimmermann, «Phased arrays-part II: implementations, applications, and future trends», *IEEE Transactions on Microwave Theory and Techniques*, vol. 50, n°. 3, pagg. 688 –698, Mar 2002.

[4] S. Vaccaro, F. Tiezzi, D. Llorens, M. F. Rua, e C. D. G. de Oro, «Ku-Band Low Profile Antennas for Mobile Satcom», in *Advanced Satellite Mobile Systems, 2008. ASMS 2008. 4th*, 2008, pagg. 24 –28.

[5] M. Lisi, «Antenna technologies for multimedia mobile satellite communications», in *Antennas and Propagation, 2001. Eleventh International Conference on (IEE Conf. Publ. No. 480)*, 2001, vol. 1, pagg. 241 –245 vol.1.

[6] R. Baggen, S. Vaccaro, e D. L. del Rio, «Design Considerations for Compact Mobile Ku-Band Satellite Terminals», in *The Second European Conference on Antennas and Propagation, 2007. EuCAP 2007*, 2007, pagg. 1 –5.

[7] L. Baggen, S. Vaccaro, D. Llorens del Rio, e G. Langgartner, «Compact phased arrays for mobile terminals», in *Semiconductor Conference (CAS), 2010 International*, 2010, vol. 01, pagg. 3 –9.

[8] S. H. Son, U. H. Park, S. I. Jeon, e C. J. Kim, «Mobile antenna system for Ku-band satellite Internet service», in *Vehicular Technology Conference, 2005. VTC 2005-Spring. 2005 IEEE 61st*, 2005, vol. 1, pagg. 234 – 237 Vol. 1.

[9] Flexwin Consortium, «www.flexwin.eu».

[10]Ansys, «Ansoft HFSS, Canonsburg, PA, ver. 14», 2012.

[11] V. Valenta, M. Kaynak, G. Liu, A. Ulusoy, T. Purtova, A. Trasser, e H. Schumacher, «From enabling technology to applications: reconfigurable SiGe BiCMOS ICs with fully integrated RF MEMS switches for millimetre wave transceivers», *ESA, Microwave Technology and Techniques Workshop*, 2012.